

Supporting Information

Kucharzewska et al. 10.1073/pnas.1220998110

SI Materials and Methods

Cell Lines and Cell Culture. U87 MG and LN18 cell lines established from tumors of glioblastoma multiforme (GBM) patients were purchased from American Type Culture Collection. U118 MG GBM cells were obtained from Cell Lines Service. All GBM cell lines were cultured in Dulbecco's modified Eagle medium (DMEM) (PAA Laboratories) supplemented with 10% (vol/vol) FBS. Primary human umbilical vein endothelial cells (HUVECs) were obtained from Lonza and cultured in endothelial basal medium (EBM) supplemented with 10% (vol/vol) FBS, 10 ng/mL epidermal growth factor (EGF), and 1 μ g/mL hydrocortisone. Human brain microvascular ECs (HBMECs) and human brain vascular pericytes (HBVPs) were purchased from 3H Biomedical. HBMECs were cultured in EC medium (3H Biomedical) supplemented with 5% (vol/vol) FBS and EC growth supplement. HBVPs were cultured in pericyte medium (3H Biomedical) supplemented with 2% (vol/vol) FBS and pericyte growth supplement. All media were supplemented with 2 mM L-glutamine, 100 U/mL penicillin, and 100 μ g/mL streptomycin. ECs and HBVPs at passages 2–6 were used for experiments. Routine culture was done in a humidified incubator maintained at 37 °C with 5% CO₂ and 95% air. For hypoxia experiments, cells were incubated in a humidified 5% CO₂ In Vivo₂ Hypoxia Work station 400 (Ruskin Technology Ltd) set at 37 °C and 1% O₂.

Exosome Isolation. Exosomes were isolated by differential centrifugation. To this end, U87 MG cells were cultured in DMEM supplemented with 1% BSA at normoxic or hypoxic conditions. Conditioned media were collected from 48-h cell cultures and centrifuged at 300 \times g, 4 °C for 5 min to eliminate cell debris. Supernatant fractions were further centrifuged at 16,500 \times g, 4 °C for 30 min. Exosomes were then pelleted by ultracentrifugation at 100,000 \times g, 4 °C for 2 h, followed by washing with PBS and ultracentrifugation at 100,000 \times g, 4 °C for 2 h. The washing step was repeated once for a total of two washes. Exosomes were resuspended in PBS for functional assays or used for protein or RNA isolation. For the isolation of mouse and human plasma-derived exosomes, peripheral blood was collected in tubes with EDTA and BD Vacutainer tubes with sodium heparin, respectively, and spun at 2,000 \times g at room temperature for 15 min to obtain plasma. Plasma was diluted at least 1:4 with PBS and spun at 5,000 \times g, 4 °C for 15 min. Exosomes were pelleted by ultracentrifugation at 100,000 \times g, 4 °C for 2 h. Exosome pellets were washed once in a large volume of PBS, centrifuged at 100,000 \times g, 4 °C for 2 h, and used for further molecular analyses.

Transmission Electron Microscopy. For negative staining, isolated exosomes were washed in TBS twice, pelleted by ultracentrifugation at 100,000 \times g, 4 °C for 2 h, and fixed in 2.5% glutaraldehyde (vol/vol) in cacodylate buffer. Exosomes were adsorbed onto 400 mesh carbon-coated copper grids and stained with 0.75% uranyl formate (wt/vol) as described (1). Samples were observed in a FEI Tecnai G2 Spirit transmission electron microscope (North America NanoPort) operated at 60 kV accelerating voltage. Images were recorded with an Olympus SIS Veleta CCD camera.

Western Blot Analysis. Exosomes and cells were lysed with radioimmunoprecipitation assay (RIPA) buffer (10 mM Tris-HCl at pH 7.4, 150 mM NaCl, 1 mM EDTA, 0.1% SDS, 1% Triton X-100, and 1% sodium deoxycholate) supplemented with Complete Protease Inhibitor Mixture tablets (Roche Diagnostics). For antibodies requiring nondenaturing conditions (CD63 and

CD81) samples were lysed in Triton X-100 lysis buffer (20 mM Tris-HCl at pH 8.0, 137 mM NaCl, 1% Triton X-100, and 2 mM EDTA) supplemented with Complete Protease Inhibitor Mixture tablets. Protein concentration was determined by using the BCA Protein Assay Kit (Pierce), and equal amounts of proteins were separated by SDS/PAGE and transferred to PVDF membranes (Pall Corporation). After blocking, membranes were probed with the following primary antibodies: anti-CD63 (Abcam; ab8219), anti-CD81 (Abcam; 23505), anti-flotillin (Abcam; 41927), anti- α -tubulin (Abcam; 7291), anti-GM130 (BD Transduction Laboratories; 610823), anti-LAMP (lysosome-associated membrane protein) 1 (Abcam; 19294), anti-insulin-like growth factor binding protein (IGFBP) 3 (GroPep; PAAJ1), anti-lysyl oxidase (LOX) (Santa Cruz Biotechnology; sc-32409), anti-N-myc downstream regulated 1 (NDRG1) (R&D Systems; AF5209), anti-adrenomedullin (ADM) (R&D Systems; AF6108), anti-IL8 (R&D Systems; AF208), anti-caveolin1 (CAV1) (Abcam; 2910), anti-HIF1 α (Abcam; ab1), anti-hypoxia inducible factor (HIF)2 α (Novus Biologicals; NB100-132), anti-phospho-ERK1/2 (Sigma; M8159), anti-ERK (Cell Signaling Technology; 9102), anti-phospho-AKT (Cell Signaling Technology; 9271), anti-AKT (Cell Signaling Technology; 9272), anti-phospho-p38 (p38 mitogen-activated protein kinase) (Cell Signaling Technology; 9215), anti-p38 (Cell Signaling Technology; 9212), anti-phospho-FAK (Cell Signaling Technology; 3281), and anti-FAK (focal adhesion kinase) (Cell Signaling Technology; 3285). Protein was visualized by using horseradish peroxidase (HRP)-conjugated secondary antibodies (Amersham International) and ECL Western blotting substrate (Pierce). The intensities of immunoreactive bands were quantified by densitometry using ImageJ software (National Institutes of Health).

Membrane-Based Antibody Arrays. U87 MG cells and corresponding exosomes as well as plasma-derived exosomes were lysed in RIPA buffer supplemented with Protease Inhibitor Mixture tablets (Roche Diagnostics). Total protein from U87 MG cells and exosomes (400 μ g) and from plasma-derived exosomes (300 μ g) was analyzed by using the Human Angiogenesis Antibody Array (R&D Systems). The arrays were scanned and quantified with Image J software (National Institutes of Health). Presented data show fold change of relative protein levels (normalized to array reference marked with red box) in GBM patient exosomes compared with age- and sex-matched control subject exosomes (Fig. 1), and in exosomes from hypoxic compared with normoxic GBM cells as well as tumor-bearing compared with tumor-free mice (Fig. 3). For analysis of conditioned media from ECs stimulated with exosomes, HUVECs were seeded in 20-cm² dishes and grown in the presence or absence of exosomes derived from hypoxic U87 MG cells at 40 μ g/mL in serum-free EBM at hypoxic conditions. After 24-h incubation, conditioned media were collected and centrifuged at 1,000 \times g, 4 °C for 5 min. Half of the conditioned medium from ECs stimulated with exosomes was additionally spun at 100,000 \times g, 4 °C for 70 min, resulting in a soluble fraction [endothelial cell (EC) + GBM cell-derived exosomes (Exo CM Sol)]. Obtained samples were analyzed with Human Cytokine Antibody arrays (R&D Systems), scanned with ImageJ, and quantified as described above. For analysis of activation of receptor tyrosine kinases (RTKs) in ECs upon stimulation with U87 MG cell-derived exosomes, HUVECs were seeded in 60-cm² dishes, starved in serum-free EBM overnight, and then stimulated with hypoxic

exosomes (10 and 40 $\mu\text{g/mL}$) for 10 min. Total protein from HUVECs (100 μg) was analyzed by using the Human Phospho-RTK Antibody Array (R&D Systems). The arrays were scanned and quantified with ImageJ software. All of the arrays were performed according to the manufacturer's recommendations.

Gene Expression Microarray Analysis. Total RNA was extracted with TRIzol Reagent (Life Technologies) and quantified by using a Nanodrop ND-1000 spectrophotometer (Saven Werner). RNA integrity was verified on an Agilent 2100 Bioanalyzer. Microarray experiments were performed at Swegene Center for Integrative Biology at Lund University Genomics Center at Lund University, Sweden, using one Illumina HumanHT-12 v3 Expression BeadChip. Three independent preparations of normoxic and hypoxic U87 MG cells and corresponding exosomes were analyzed on the 12 arrays on the BeadChip. Data filtration and normalization were performed by using BASE2 (2), and subsequent analyses on transcripts showing a detection *P* value below 0.01 were performed by using the R statistical programming environment (www.r-project.org). Hypoxia-mediated gene expression changes, calculated as the ratio of mean hypoxia intensity divided by mean normoxia intensity across the triplicate assays, were determined for cells and exosomes separately. Gene lists ranked by the hypoxia/normoxia ratio were used as input for gene set enrichment analysis (3) by using the predefined Curated gene set collection. The MeV software was used to extract transcripts differentially expressed between normoxic and hypoxic exosomes.

Quantitative Real-Time PCR. cDNA synthesis from total RNA was performed by using SuperScript III First-Strand Synthesis System (Life Technologies). cDNA was used for PCR based on SYBR Green I chemistry (Sigma) in an ABI PRISM 7900 HT machine (Applied Biosystems). The primers used were as follows: ADM, forward 5'-AGAGGGAAGTCCGGATGTC-3' and reverse 5'-CCTTGTCCTTACTGTGAAGTGG-3'; β -actin, forward 5'-AGCACAGAGCCTCGCCTTT-3' and reverse 5'-GGAATCCTTCTGACCCATGC-3'; BCL2/adenovirus E18 19-kDa interacting protein 3 (BNIP3), forward 5'-GGCTCCTGGGTAGAACTGC-3' and reverse 5'-CCCTGTTGGTATCTTGTGGTG-3'; endothelial differentiation-related factor (EDF) 11, forward 5'-TTCCAA-GAAATGGGCTGCT-3' and reverse 5'-CCGTCCGCTCTCATAGTCC-3'; glucose transporter 1 (GLUT1), forward 5'-GGCAAGTCCCTTGAGATGCT-3' and reverse 5'-CGGGATGAAGATGATGCTC-3'; Inhibitor of DNA binding 2, forward 5'-CTGACCACCCTCAACACG-3' and reverse 5'-AACTTGTCCTCCTTGTAAGATG-3'; IGFBP3, forward 5'-TCCAAGCGGGAGACAGAATA-3' and reverse 5'-ATCCACACACCA-GCAGAAGC-3'; LOX, forward 5'-CTACTACATCCAGGCG-TCCAC-3' and reverse 5'-ACTCTTTGGGAAATCTGAGC-3'; NDRG1, forward 5'-GTGGAGAAAGGGGAGACCAT-3' and reverse 5'-AGTTGAAGAGGGGGTTGTAGC-3'; plasminogen activator inhibitor-1 (PAI1), forward 5'-CTCTCTCT-GCCCTACCAAC-3' and reverse 5'-CGGTCATTCCAGGTTCTCTA-3'; procollagen-lysine 2-oxoglutarate 5-dioxygenase 2 (PLOD2), forward 5'-CGAGCATCCACAGATAAAT-3' and reverse 5'-ATTCCATCACCACCTCTCCAT-3'; VEGFA (isoform A), forward 5'-AGCCTTGCCCTTGCTGCTCTA-3' and reverse 5'-GTGCTGGCCTTGGTGAGG-3'. β -actin and EDF1, which were stable between normoxic and hypoxic conditions, were used as reference genes. All reactions were run in triplicate, and relative expression was calculated by using the comparative Ct method ($2^{-[\Delta\Delta\text{Ct}]}$).

Exosome Uptake. Exosomes were labeled with PKH67 Green Fluorescent labeling kit (Sigma) as recommended by the manufacturer. Subconfluent HUVECs and HBVPs were incubated with 5 $\mu\text{g/mL}$ labeled exosomes for varying times at serum-free

conditions, trypsinized, washed with PBS supplemented with 1% BSA, and analyzed by flow cytometry on a FACSCalibur instrument integrated with Cell-Quest software (BD Biosciences). Alternatively, HUVECs and HBVPs were seeded on chamber slides and incubated with labeled exosomes (5 $\mu\text{g/mL}$) for 90 min and subsequently analyzed by using Zeiss LSM710 confocal scanning equipment with a C-Apochromat 63 \times /1.20 W M27 objective.

Cell Proliferation Assay. Subconfluent ECs were incubated with varying concentrations of normoxic or hypoxic glioma cell-derived exosomes or GBM patient-derived exosomes at hypoxic conditions for a total of 72 h. During the last 24 h of incubation, cells were cultured in the presence of 6.25 $\mu\text{Ci/mL}$ [^3H]-thymidine (PerkinElmer). HBVPs and U87 MG cells were grown in conditioned medium collected from HUVECs cultured in the presence or absence of exosomes (40 $\mu\text{g/mL}$) from hypoxic U87 MG cells for 24 h. The cells were cultured in the presence of 6.25 $\mu\text{Ci/mL}$ [^3H]-thymidine during the last 3 h of incubation. The amount of incorporated [^3H]-thymidine was determined by Beckman Coulter LS6500 liquid scintillation counting.

Survival Assay. Subconfluent ECs were incubated with varying concentrations of normoxic or hypoxic glioma cell-derived exosomes in serum-free media at hypoxia for 48 h. Floating and trypsinized cells were pooled, labeled with 7-amino-actinomycin D (7-AAD) (Calbiochem) to detect apoptotic/necrotic cells, and analyzed by flow cytometry on a FACSCalibur instrument integrated with Cell-Quest software. Viability of HUVECs after 48-h incubation in serum-free media at hypoxia in the presence or absence of exosomes isolated from GBM patient's plasma was determined by the MTT assay (Sigma) according to the manufacturer's recommendations.

Cell Migration Assay. HBVPs or U87 MG cells were starved in serum-free media overnight. Cells (5×10^4) were added in serum-free media to the top chambers of 8- μm pore cell culture inserts (BD Biosciences) placed in a 24-well plate. Cells were incubated at 37 $^\circ\text{C}$ for 6 h to allow cell migration toward exosomes, serum-free medium, or conditioned media collected from HUVECs grown in the presence or absence of exosomes derived from hypoxic U87 MG cells. Migrated cells attached to bottom membrane were fixed, stained with crystal violet, and counted in five random fields under the microscope (Axiovert 40C, 20 \times objective; Carl Zeiss).

Matrigel Tube Formation Assay. ECs were pretreated with normoxic or hypoxic exosomes (10 $\mu\text{g/mL}$) for 24 h and were then seeded into a growth factor-reduced BD Matrigel (BD Bioscience) precoated 96-well plate at 5×10^4 cells per well in EBM supplemented with 5% (vol/vol) FBS and EC growth supplement. EC tube formation was captured 20 h after seeding (Axiovert 40C microscope, 10 \times objective; Carl Zeiss). The angiogenic property was assessed by counting the number of tubes per microscopic field.

Ex Vivo Mouse Aortic Ring Sprouting Assay. Thoracic aortas were isolated from nonobese diabetes/SCID mice and immediately placed in EBM supplemented with 1% L-glutamine, 100 U/mL penicillin G, 100 $\mu\text{g/mL}$ streptomycin, and 0.25 $\mu\text{g/mL}$ amphotericin B. Fibroadipose tissue was carefully removed under a dissecting microscope. The aortic pieces were placed in fresh EBM in the presence or absence of normoxic or hypoxic exosomes (25 $\mu\text{g/mL}$) and incubated for 24 h. Subsequently, aortic pieces were embedded in growth factor-reduced BD Matrigel and overlaid with EBM supplemented with 2% (vol/vol) mouse serum, 1% L-glutamine, 100 U/mL penicillin G, 100 U/mL streptomycin, 0.25 $\mu\text{g/mL}$ amphotericin B and normoxic or hypoxic exosomes (25 $\mu\text{g/mL}$), and incubated in a 5% CO_2 hu-

modified incubator at 37 °C for 7 d. The number of microvessel sprouts and their length were determined by using an inverted microscope equipped with a 20× objective (Axiovert 40C; Carl Zeiss). Images of aortic pieces were captured by using a Leica MZ 12.5 stereomicroscope and DFC280 camera (10× magnification).

Laser-Capture Microdissection. U87 MG xenograft and human GBM tumor optimal cutting temperature medium (O.C.T.) sections (10 μm) were mounted onto membrane slides (MembraneSlide 1.0 PEN NF; Zeiss) before laser-capture microdissection (LCM) or onto poly-lysine coated slides for GLUT1 immunohistochemical analysis. LCM sections were fixed with RNase-free ice-cold 70% (vol/vol) ethanol for 1 min, followed by quick staining in hematoxylin supplemented with RNase inhibitor SUPERaseIn (Ambion). Slides were washed with RNase-free PBS and increasing ice-cold ethanol concentrations (70%, 95%, and 100%) (vol/vol) and stored in sterile 50-mL tubes before LCM using the PALM system from Zeiss. Hypoxic tumor regions were identified by GLUT1 staining present on the neighboring tumor section. Excised normoxic and hypoxic tissue samples (approximately 2 μm²) were dissolved in 100 μL of lysis solution provided with RNeasy-Micro kit (Ambion), and RNA isolation was performed according to the manufacturer's instructions. RNA samples were treated with DNase I (Ambion), and their concentration was determined with RiboGreen RNA Quantification kit (Invitrogen). Equal amounts of RNA from normoxic and hypoxic samples were used for cDNA synthesis, followed by quantitative RT-PCR (qRT-PCR) analysis.

Immunohistochemistry. Cryopreserved O.C.T. tumor sections (10 μm), corresponding to specimens used for LCM analysis, were fixed with ice-cold 95% (vol/vol) ethanol for 1 min, dried at room temperature, blocked with 5% (vol/vol) FBS in PBS for 1 h, and incubated with primary anti-GLUT1 antibody (Abcam; 40084) at 4 °C overnight. The paraffin-embedded U87 MG xenograft

tumor sections (5 μm) were deparaffinized, rehydrated, and subjected to antigen retrieval in sodium citrate buffer (pH 6.0) at 95 °C to 100 °C. Hematoxylin/eosin (H&E) staining was performed according to common methods. For Ki67 staining, sections were blocked with 3% (vol/vol) H₂O₂ for 10 min, followed by washing, blocking with 5% (vol/vol) FBS in PBS for 1 h, and incubation with primary anti-Ki67 antibody (Abcam; 15580) at 4 °C overnight. After washing, GLUT1 and Ki67 stained sections were incubated with HRP-conjugated secondary antibody for 1 h at room temperature, and then antigen sites were visualized with the DAB-Plus Substrate Kit (Invitrogen). Sections stained for Ki67 were additionally counterstained with hematoxylin before drying and mounting with PermaFluor (Beckman Coulter). Negative controls were stained in parallel with secondary antibody alone. Sections were analyzed by using Mirax Midi Scanner integrated with Mirax Viewer 1.11 software (Carl Zeiss).

Immunofluorescence. The paraffin-embedded U87 MG xenograft tumor sections (5 μm) were prepared for staining as described above. The paraffin-embedded human GBM tumor sections (5 μm) were deparaffinized, rehydrated, and subjected to antigen retrieval in EnVision Flex Target Retrieval Solution High pH (Dako) by using PTLINK method (Dako). After blocking with 5% (vol/vol) FBS in PBS for 1 h, tumor sections were incubated with primary antibodies to CD31 (Dako; M0823), α-SMA (Abcam; 5694), CAV1, IL-8, and GLUT1 at 4 °C overnight. After washing, tissue sections were incubated with fluorophore-conjugated secondary antibody for 1 h at room temperature. Negative controls were stained in parallel with secondary antibody alone. Sections were counterstained with Hoechst 33342 nuclear stain, mounted with PermaFluor (Beckman Coulter), and analyzed by using Axio Observer.Z1 HB 100 fluorescence microscope equipped with a 20× water objective (Carl Zeiss).

1. Abdillahi SM, Balvanović S, Baumgarten M, Mörgelin M (2012) Collagen VI encodes antimicrobial activity: novel innate host defense properties of the extracellular matrix. *J Innate Immun* 4(4):371–376.
2. Vallon-Christersson J, Nordborg N, Svensson M, Häkkinen J (2009) BASE—2nd generation software for microarray data management and analysis. *BMC Bioinformatics* 10:330.

3. Subramanian A, et al. (2005) Gene set enrichment analysis: A knowledge-based approach for interpreting genome-wide expression profiles. *Proc Natl Acad Sci USA* 102(43):15545–15550.

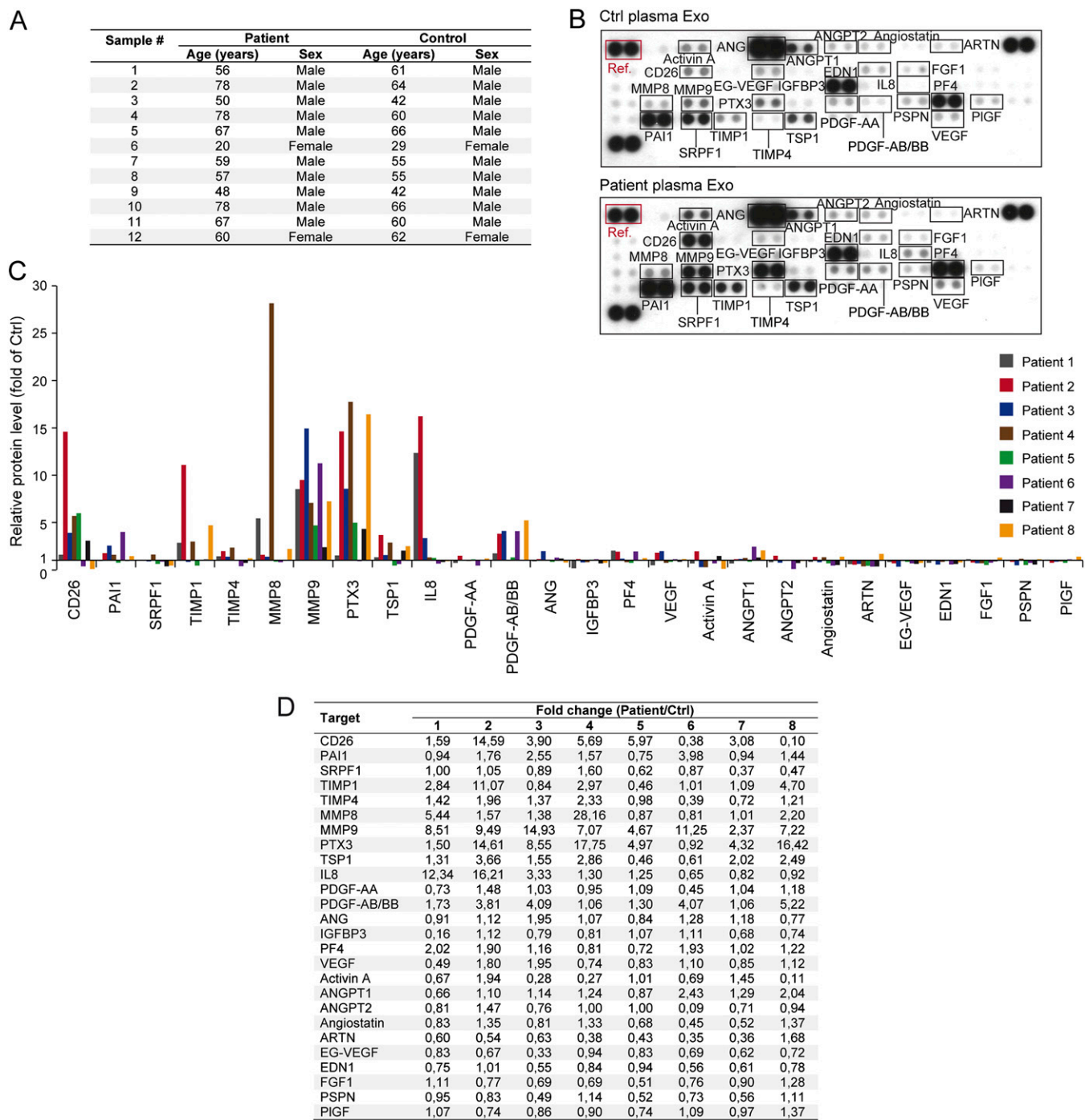


Fig. S1. GBM patient plasma exosomes have increased levels of hypoxia-regulated proteins involved in tumor development. (A) Characteristics of GBM patients and corresponding healthy controls. (B) Antibody array analyses of exosomes from GBM patients (patient plasma Exo) and age- and sex-matched control subjects (Ctrl plasma Exo). Shown is array data from a representative patient-control experiment. Proteins present at significant levels are marked by black boxes. (C and D) Presented data show fold change of relative protein levels (normalized to array reference) in GBM patient exosomes compared with matched control subject exosomes.

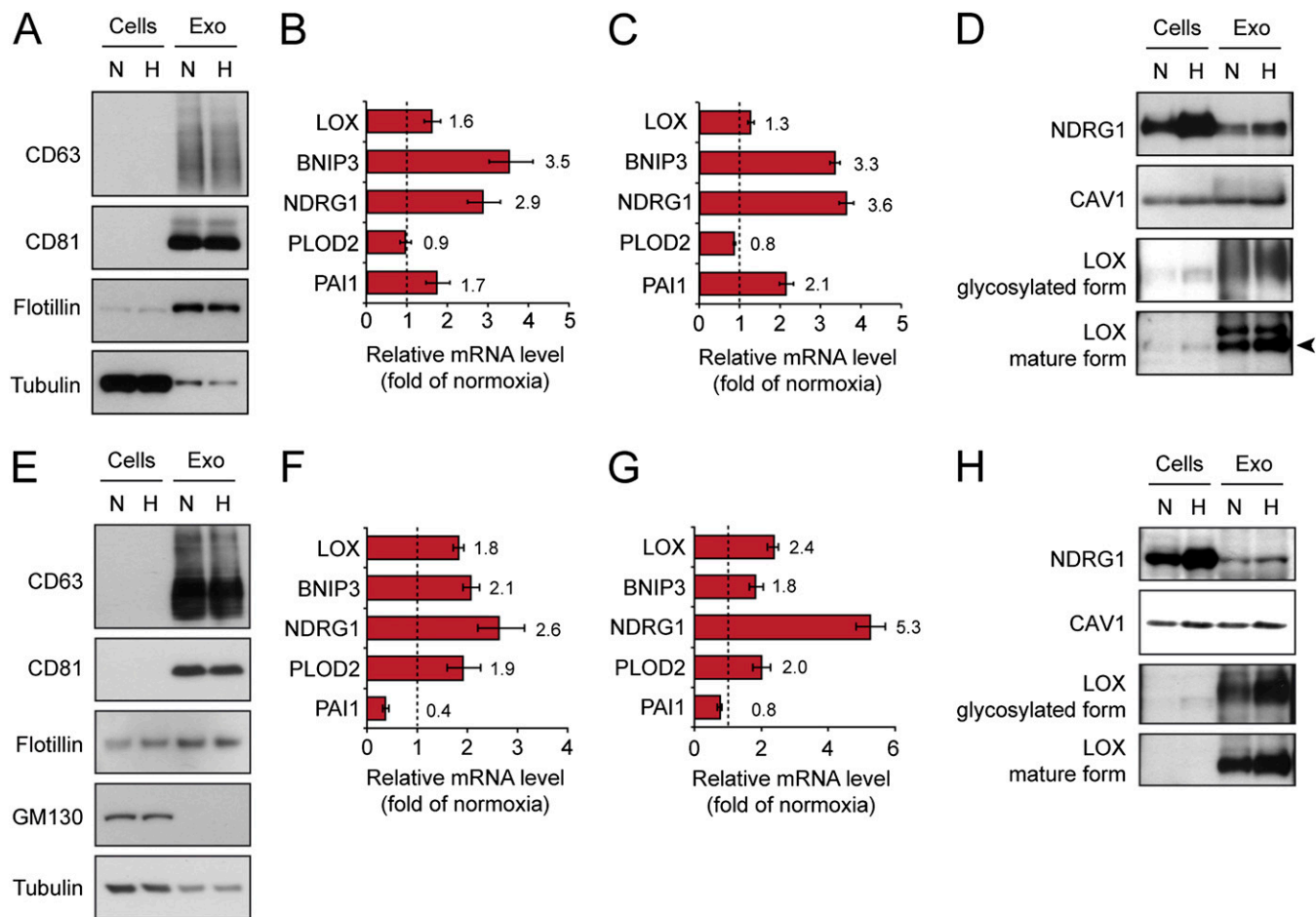


Fig. 53. The hypoxic profile of exosomes reflects the hypoxic signaling response of GBM cells. Normoxic (N) and hypoxic (H) U118 MG (A) and LN18 (E) cells and corresponding exosomes were analyzed by immunoblotting demonstrating the enrichment of the tetraspanins CD63 and CD81, the raft marker flotillin, and the relative depletion of tubulin in exosomes compared with cell lysates. Hypoxic induction of indicated mRNAs in exosomes from U118 MG (B) and LN18 (F) GBM cells by qRT-PCR. Data are presented as fold increase in hypoxic compared with normoxic exosomes \pm SD and are representative of three independent experiments. Values beside bars indicate fold change in hypoxic exosomes. (C) and (G) Similar experiment as in (B) and (F) performed with the corresponding GBM donor cells. Equal amount of total protein from normoxic (N) or hypoxic (H) U118 MG (D) and LN18 (H) GBM cells and corresponding exosomes (Exo) were analyzed for the indicated proteins by Western blotting. Arrow-head in (D) denotes mature form of LOX protein.

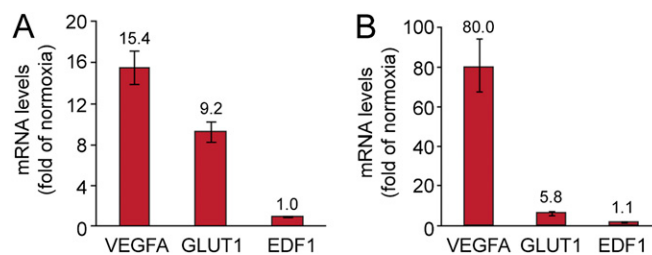


Fig. 54. Validation of laser-capture microdissection procedure of GBM tumors. Frozen sections of human GBM xenografts (A) and GBM patient tumors (B) were stained with GLUT1 antibody for the definition of hypoxic regions (Fig. 2). LCM was performed on neighboring, hematoxylin-stained sections. Total RNA was isolated from cutout normoxic and hypoxic tumor regions and further analyzed for VEGFA, GLUT1, and EDF1 transcripts by qRT-PCR analysis. Data are expressed as fold increase of transcript levels in hypoxic compared with normoxic tumor regions \pm SD and are representative of three independent experiments. Values above bars indicate fold change in hypoxic tumor regions.

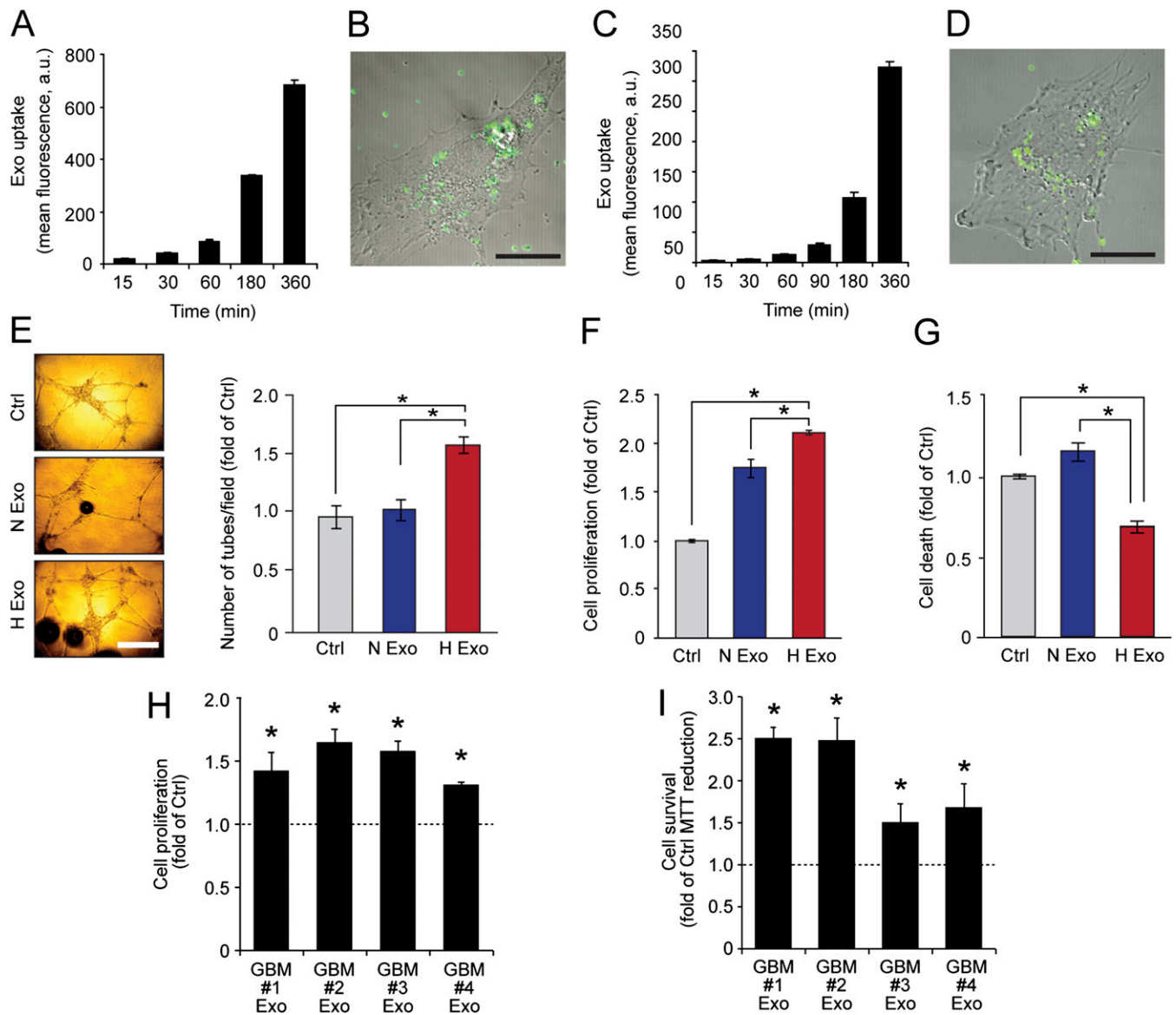


Fig. 55. GBM cell-derived exosomes are internalized by primary ECs and pericytes. (A and C) Flow cytometry analysis of HUVECs (A) and human brain vascular pericytes (C) incubated with PKH67-labeled exosomes (Exo) (5 $\mu\text{g}/\text{mL}$) for the indicated times showing time-dependent uptake of exosomes. Data are mean \pm SD, $n = 3$. (B and D) Confocal microscopy images illustrating the internalization of PKH67-labeled exosomes (green) by ECs (B) and pericytes (D) into endocytic structures after 90 min of incubation. (Scale bar: 20 μm .) Role of exosomes in hypoxia-dependent signaling between malignant cells and microvascular ECs. (E) Primary human brain microvascular ECs (HBMECs) were cultured for 24 h in the absence (Ctrl) or presence of exosomes (10 $\mu\text{g}/\text{mL}$) derived from normoxic (N) or hypoxic (H) GBM cells, and then grown on Matrigel for 16 h. (Left) Representative photomicrographs of EC tube morphology from the different treatment groups. (Scale bar: 500 μm .) (Right) Quantitative analysis of tubes/microscopic field presented as the mean \pm SD, $n = 4$ per group. $*P < 0.05$. Hypoxia potentiates exosomal stimulation of EC proliferation and survival. (F) HBMECs were cultured in the absence (Ctrl) or presence of exosomes (1 $\mu\text{g}/\text{mL}$) derived from N or H GBM cells for a total period of 72 h, and cells were assessed for proliferation by [^3H]-thymidine incorporation. (G) HBMECs were cultured in the absence (Ctrl) or presence of N or H exosomes (50 $\mu\text{g}/\text{mL}$) for 48 h, and cells were assessed for cell death by 7-AAD staining. Data are presented as fold of untreated, control cells, and are the mean \pm SD, $n = 4$. $*P < 0.05$. GBM patient-derived exosomes stimulate EC proliferation and survival. (H) HUVECs were cultured in the presence of exosomes derived from four different GBM patients for a total period of 72 h, and cells were assessed for proliferation by [^3H]-thymidine incorporation. (I) Viability of HUVECs after 48 h of incubation in serum-free medium at hypoxia in the presence or absence of patient-derived exosomes was determined by the 3-(4,5-dimethylthiazol-2-yl)-2,5-diphenyl tetrazolium bromide assay. Data are presented as fold of untreated, control cells, and are the mean \pm SD, $n = 4$. $*P < 0.05$.

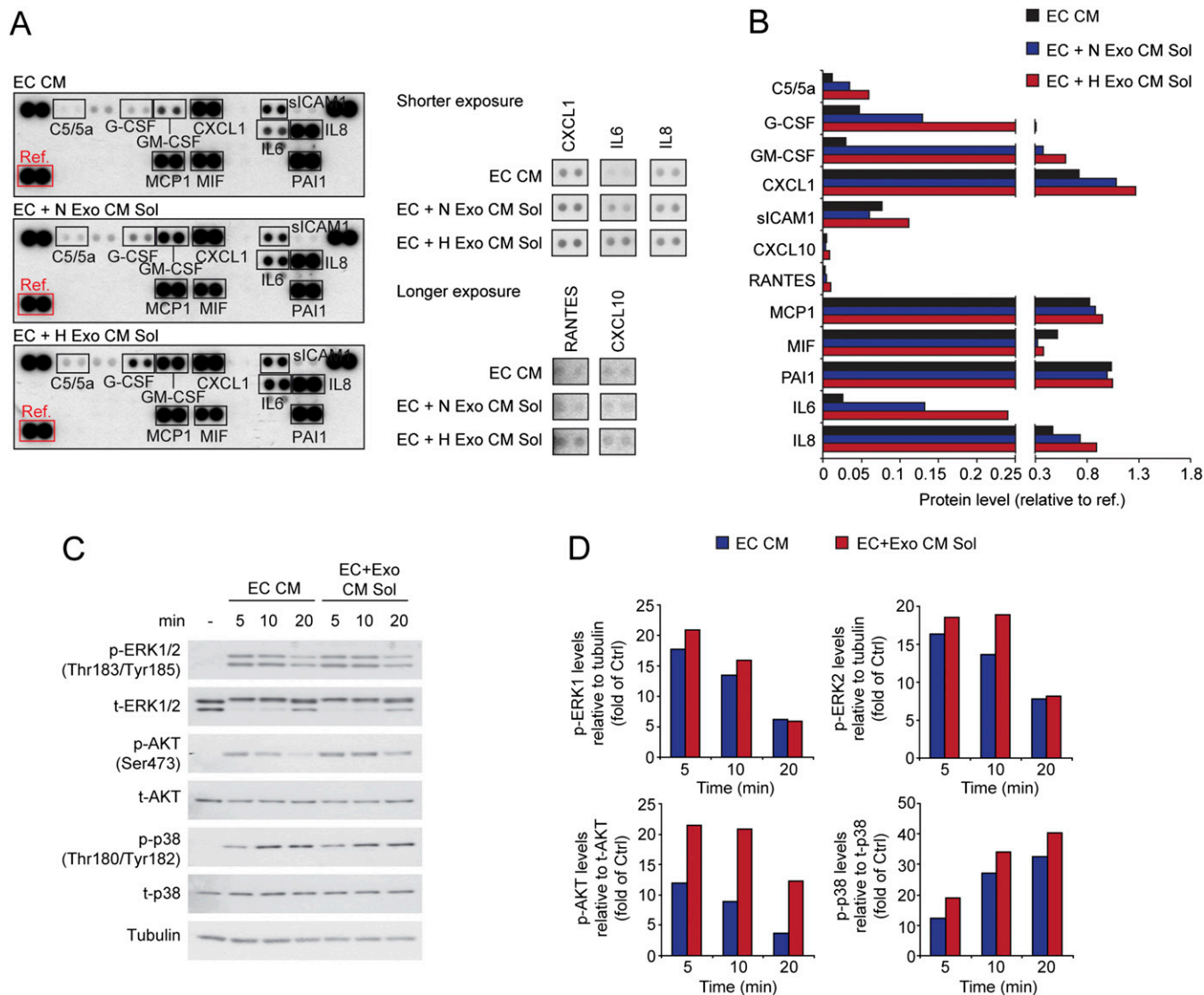


Fig. S7. GBM cell-derived exosomes trigger the secretion of proangiogenic proteins and paracrine pericyte signaling activation by ECs. (A and B) Hypoxic ECs were preconditioned for 24 h without (conditioned medium from untreated ECs; EC CM) or with exosomes (40 μ g/mL) from normoxic (EC + N Exo CM Sol) or hypoxic (EC + H Exo CM Sol) GBM cells, and conditioned medium was collected and processed into an exosome-free, soluble fraction. Angiogenic protein expression profiles of CM were analyzed by antibody arrays. (A) Array data from a representative experiment. Selected target proteins are displayed at various exposure times to better visualize the intensities. (B) The arrays were scanned and quantified with ImageJ software. Data are representative of two independent experiments and represent relative protein levels (normalized to array reference). (C) The soluble, exosome-free fraction of CM isolated from ECs preconditioned with hypoxic exosomes (EC + Exo CM Sol) exhibited increased PI3K/AKT signaling activation in primary human brain vascular pericytes compared with CM from control ECs without exosome treatment (EC CM). CM collected from ECs were incubated with pericytes for the indicated time periods, followed by immunoblotting of pericyte lysates for phosphorylated and total ERK1/2, AKT, and p38 kinases. (D) The immunoblots shown in C were scanned and quantified with ImageJ software. Data are representative of two independent experiments and represent fold change of relative phosphorylated protein levels in pericytes stimulated with EC CM or EC + Exo CM Sol compared with untreated pericytes (Ctrl).

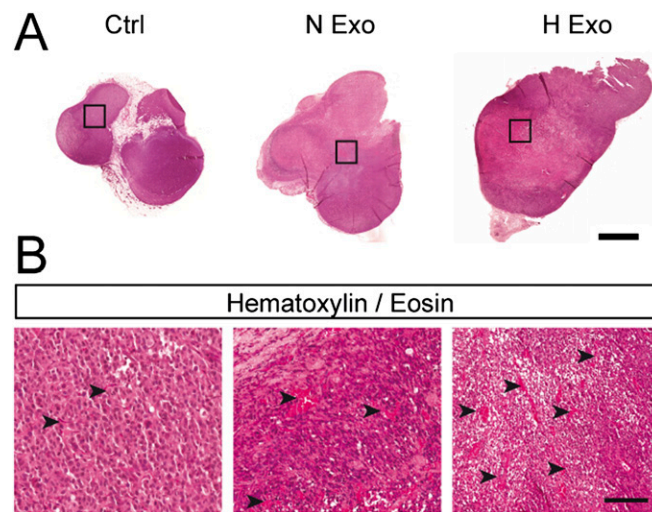


Fig. 58. Hypoxic exosomes accelerate tumor angiogenesis and growth. Human GBM xenografts were established in SCID mice with or without exosomes (1 $\mu\text{g}/\text{mL}$) from normoxic (N Exo) or hypoxic (H Exo) GBM cells. Tumors from the different treatment groups were evaluated by immunohistochemistry. (A) Representative photomicrographs of tumors from control mice and the respective treatment groups obtained at 1 \times magnification. (B) Arrowheads indicate blood vessels. (Scale bars: A, 2 mm; B, 100 μm .)

Table S1. Transcripts with significantly different expression levels in normoxic and hypoxic exosomes

mRNA	Description	Fold change
IGFBP3	Insulin-like growth factor binding protein 3	10.0
LOX	Lysyl oxidase	6.2
HIG2	Hypoxia inducible protein 2	5.3
ANKRD37	Ankyrin repeat domain 37	4.0
NDRG1	N-myc downstream regulated 1	3.9
PPP1R3C	Protein phosphatase 1 regulatory (inhibitor) subunit 3C	2.9
ERRFI1	ERBB receptor feedback inhibitor 1	2.8
MT3	Metallothionein 3	2.8
SLC6A10P	Solute carrier family 6 (neurotransmitter transporter, creatine)	2.7
ZP1	Zona pellucida glycoprotein 1	2.6
ADM	Adrenomedullin	2.2
LIMS1	LIM and senescent cell antigen-like domains 1	2.1
ID2	Inhibitor of DNA binding 2	2.0
LRIG1	Leucine-rich repeats and Ig-like domains 1	2.0
STC2	Stanniocalcin 2	2.0
INSIG2	Insulin induced gene 2	2.0
PLOD2	Procollagen-lysine 2-oxoglutarate 5-dioxygenase 2	2.0
DPYSL4	Dihydropyrimidinase-like 4	2.0
PAI1/SERPINE1	Plasminogen activator inhibitor-1	2.0
MTMR4	Myotubularin related protein 4	2.0
CDCA2	Cell division cycle associated 2	1.9
PFKFB4	6-Phosphofructo-2-kinase/fructose-2,6-bisphosphatase 4	1.9
WFDC3	WAP four-disulfide core domain 3	1.9
BNIP3	BCL2/adenovirus E18 19kDa interacting protein 3	1.8
HSPB3	Heat shock 27kDa protein 3	1.8
DSCR1	Regulator of calcineurin 1	1.8
SYTL2	Synaptotagmin-like 2	1.7
ISG20	IFN stimulated exonuclease gene 20kDa	1.7
ENO2	Enolase 2 (gamma, neuronal)	1.7
SNTA1	Syntrophin, alpha 1	1.6
H1FO	H1 histone family, member 0	1.6
GBE1	Glucan (1,4-alpha-), branching enzyme 1	1.6
PGK1	Phosphoglycerate kinase 1	1.5
SHB	Src homology 2 domain containing adaptor protein B	1.5
LDHA	Lactate dehydrogenase A	1.5
ZNF395	Zinc finger protein 395	1.5
WDR45L	WD repeat domain phosphoinositide-interacting protein 3	1.5
CDC2L6	Cell division cycle 2-like 6	1.5
RALGDS	Ral guanine nucleotide dissociation stimulator	1.5
ACADVL	Acyl-CoA dehydrogenase, very long chain	1.4
MRPL23	39S ribosomal protein L23, mitochondrial	1.4
MST4	Mammalian STE20-like protein kinase 4	1.3
ALKBH5	Alkylation repair homolog 5	1.3
PTPLB	Protein tyrosine phosphatase-like, member b	1.2
PPIE	Peptidylprolyl isomerase E	1.1
SF3B14	Splicing factor 3B, 14 kDa subunit	0.9
ZYX	Zyxin	0.9
SUMO2	Small ubiquitin-related modifier 2	0.9
COPB2	Coatomer protein complex, subunit beta 2	0.9
PPHLN1	Periplin-1	0.8
RPS2	40S ribosomal protein S2	0.8
C11orf10	Chromosome 11 ORF 10	0.8
RNF24	Ring finger protein 24	0.8
C4orf34	Chromosome 4 ORF 34	0.8
NXF1	Nuclear RNA export factor 1	0.8
BOLA2	BolA homolog 2	0.8
HADH2	Hydroxysteroid (17-beta) dehydrogenase 10	0.8
RPS3	Ribosomal protein S3	0.8
C3orf60	NADH dehydrogenase [ubiquinone] 1 alpha subcomplex assembly factor 3	0.8
FKBP1A	FK506 binding protein 1A	0.8
NUPL2	Nucleoporin like 2	0.8
C3orf17	Chromosome 3 ORF 17	0.8
PTS	6-Pyruvoyltetrahydropterin synthase	0.8

Table S1. Cont.

mRNA	Description	Fold change
ATP5L	ATP synthase, H ⁺ transporting, mitochondrial Fo complex, subunit G	0.8
SFRS14	Putative splicing factor, arginine/serine-rich 14	0.8
YRDC	YrdC domain containing	0.8
BEAN	Brain-expressed protein associating with Nedd4 homolog	0.8
KIAA1160	ISY1 splicing factor homolog	0.8
ECSIT	Evolutionarily conserved signaling intermediate in Toll pathway homolog	0.8
BCCIP	BRCA2 and CDKN1A interacting protein	0.8
NDUFA1	NADH dehydrogenase (ubiquinone) 1 alpha subcomplex 1	0.8
RPS26L	Ribosomal protein S26, like	0.8
HNRNPA1	Heterogeneous nuclear ribonucleoprotein A1	0.8
CKLF	Chemokine-like factor	0.7
PIH1D1	PIH1 domain containing 1	0.7
MAPK9	Mitogen-activated protein kinase 9	0.7
PLDN	Pallidin homolog	0.7
MAT2A	Methionine adenosyltransferase II, alpha	0.7
SLC2A8	Solute carrier family 2 (facilitated glucose transporter), member 8	0.7
MPV17	MpV17 mitochondrial inner membrane protein	0.7
STX10	Syntaxin 10	0.7
SNX11	Sorting nexin 11	0.7
H3F3A	H3 histone, family 3A	0.7
UBL7	Ubiquitin-like 7 (bone marrow stromal cell-derived)	0.7
IFT43 (C14orf179)	Intraflagellar transport 43 homolog	0.7
PPP2R5C	Protein phosphatase 2, regulatory subunit B', gamma	0.7
CCDC32	Coiled-coil domain containing 32	0.7
ADAT1	Adenosine deaminase, tRNA-specific	0.7
LSM3	U6 snRNA-associated Sm-like protein LSm3	0.7
EIF2C1	Eukaryotic translation initiation factor 2C, 1	0.7
COMTD1	Catechol-O-methyltransferase domain containing 1	0.7
LPPR2	Lipid phosphate phosphatase-related protein type 2	0.7
DYNLT1	Dynein, light chain, Tctex-type 1	0.7
PFDN1	Prefoldin subunit 1	0.7
TMEM138	Transmembrane protein 138	0.7
FBXO31	F-box protein 31	0.7
BIN1	Bridging integrator 1	0.7
SSU72	SSU72 RNA polymerase II CTD phosphatase homolog	0.7
TGFBR2	Transforming growth factor, beta receptor II	0.7
SMUG1	Single-strand selective monofunctional uracil DNA glycosylase	0.7
RBMX	RNA binding motif protein, X-linked	0.7
B4GALT3	UDP-Gal:betaGlcNAc beta 1,4- galactosyltransferase, polypeptide 3	0.7
NDUFA12L	NADH dehydrogenase (ubiquinone) 1 alpha subcomplex, assembly factor 2	0.7
USF2	Upstream stimulatory factor 2	0.7
FBXL15	F-box and leucine-rich repeat protein 15	0.7
NICN1	Nicolin 1	0.7
NOLA3	NOP10 ribonucleoprotein homolog	0.7
SLC25A11	Solute carrier family 25 (mitochondrial carrier; oxoglutarate carrier), member 11	0.7
UQCRC1	Ubiquinol-cytochrome c reductase, Rieske iron-sulfur polypeptide	0.7
COX17	COX17 cytochrome c oxidase assembly homolog	0.7
C6orf1	Chromosome 6 ORF 1	0.7
CCDC12	Coiled-coil domain containing 12	0.7
KXD1 (C19orf50)	KxDL motif containing 1	0.7
RCC2	Regulator of chromosome condensation 2	0.7
EXOSC1	Exosome component 1	0.7
UBXD4	UBX domain containing 4	0.7
TSTA3	Tissue specific transplantation antigen P35B	0.6
COMMD5	COMM domain containing 5	0.6
CASP4	Caspase 4, apoptosis-related cysteine peptidase	0.6
PRKAG2	Protein kinase, AMP-activated, gamma 2 noncatalytic subunit	0.6
UBAC2	UBA domain containing 2	0.6
SLC35A5	Solute carrier family 35, member A5	0.6
ICT1	Immature colon carcinoma transcript 1	0.6
UBFD1	Ubiquitin family domain containing 1	0.6
C19orf52	Chromosome 19 ORF 52	0.6

Table S1. Cont.

mRNA	Description	Fold change
TJP1	Tight junction protein 1 (zona occludens 1)	0.6
PTRH2	Peptidyl-tRNA hydrolase 2	0.6
TNFAIP8L3	Tumor necrosis factor, alpha-induced protein 8-like 3	0.6
C9orf23	Chromosome 9 ORF 23	0.6
TBL1X	Transducin (beta)-like 1X-linked	0.6
KYNU	Kynureninase	0.6
NUDT9	Nudix (nucleoside diphosphate linked moiety X)-type motif 9	0.6
NDUFAF1	NADH dehydrogenase (ubiquinone) 1 alpha subcomplex, assembly factor 1	0.6
CACYBP	Calcyclin binding protein	0.6
TMEM237 (ALS2CR4)	Transmembrane protein 237	0.6
PET112L	Cytochrome oxidase assembly factor PET112 homolog	0.6
TLL1	Tubulin tyrosine ligase-like family, member 1	0.6
PTRH1	Peptidyl-tRNA hydrolase 1 homolog	0.6
HS1BP3	HCLS1 binding protein 3	0.6
LHX6	LIM homeobox 6	0.5
KBTBD2	Kelch repeat and BTB (POZ) domain containing 2	0.5
ELOF1	Elongation factor 1 homolog	0.5
HES6	Hairy and enhancer of split 6	0.5
ARV1	ARV1 homolog	0.5
RFTN1	Raftlin, lipid raft linker 1	0.5
CETN3	Centrin, EF-hand protein 3	0.5
ZFAND6	Zinc finger, AN1-type domain 6	0.5
CNO	Cappuccino homolog	0.4

Data were obtained with MeV and BASE2 data managing softwares. Myc, myelocytomatosis viral related oncogene.

Table S2. Angiogenesis-related proteins present in glioma cells and corresponding exosomes

Symbol	Description	Presence in cells	Presence in Exo
ANG	Angiogenin	Yes	Yes
FGF1	Fibroblast growth factor acidic	Yes	Yes
FGF2	Fibroblast growth factor basic	Yes	No
ENG	Endoglin	No	Yes
HGF	Hepatocyte growth factor	Yes	Yes
ANGPT1	Angiopoietin 1	No	Yes
IGFBP1	IGF binding protein 1	Yes	Yes
IGFBP3	IGF binding protein 3	Yes	Yes
IL1 β	Interleukin 1 beta	Yes	No
IL8	Interleukin 8	Yes	Yes
PTX3	Pentraxin 3	Yes	Yes
TIMP1	Tissue inhibitor of metalloproteinases 1	Yes	Yes
VEGFA	Vascular endothelial growth factor A	Yes	Yes
TF	Tissue factor	Yes	Yes
CD26	Dipeptidyl-peptidase 4	Yes	Yes
PAI1	Plasminogen activator inhibitor 1	Yes	Yes

EXO, exosomes.

